Development 129, 61-70 (2002)
Printed in Great Britain © The Company of Biologists Limited 2002
DEV1736

Specific heparan sulfate structures involved in retinal axon targeting

Atsushi Irie[1,*], Edwin A. Yates[2], Jeremy E. Turnbull[2,‡] and Christine E. Holt[1,‡]

[1]Department of Anatomy, University of Cambridge, Downing Street, Cambridge CB2 3DY, UK
[2]Molecular Cell Biology Research Laboratories, School of Biosciences, University of Birmingham, Edgbaston, Birmingham B15 2TT, UK
*Present address: The Tokyo Metropolitan Institute of Medical Science, Department of Biochemical Cell Research, Bunkyo-ku, Tokyo 113-8613, Japan
‡Authors for correspondence (e-mail: ceh@mole.bio.cam.ac.uk and j.e.turnbull@bham.ac.uk)

Accepted 8 October 2001

SUMMARY

Heparan sulfate (HS), a structurally diverse molecule comprising distinct sequences of sulfated disaccharide units, is abundant in the developing brain and binds to axon guidance molecules. Addition of HS to the developing *Xenopus* optic pathway causes severe targeting errors yet it is not known how the structural diversity of this molecule relates to its role in axon guidance. We have used an in vivo brain assay to identify the structural characteristics of HS that induce aberrant axon targeting. Inhibiting sulfation of endogenous HS with chlorate causes axons to bypass their target, the tectum, and treatment with chemically modified heparins reveals that 2-*O*- and 6-*O*-sulfate groups have potent bypass-inducing activity. Experiments with purified heparin saccharides show that bypass-inducing activity correlates with distinct structures, particularly those containing a combination of 2-*O*- and 6-*O*-sulfate groups. Taken together the results indicate that specific sequences, rather than gross structural composition, are critical for activity. In situ hybridisation revealed that HS 6-*O*-sulfotransferase is regionally expressed along the border of the dorsal optic tract whereas 2-*O*-sulfotransferase is expressed broadly. Our results demonstrate that specific HS sequences are essential for regulating retinotectal axon targeting and suggest that regionalised biosynthesis of specific HS structures is important for guiding axons into the tectum.

Key words: Axon guidance, Glycosaminoglycan, Heparan sulfate, Retinal axon, Sulfotransferase, *Xenopus*.

INTRODUCTION

Heparan sulfate proteoglycans (HSPGs) are abundant cell-surface molecules that consist of a core protein and highly sulfated glycosaminoglycan (GAG) sugar chains (Kjellen and Lindahl, 1991; Yanagishita and Hascall, 1992; David, 1993). HS chains bind to various extracellular molecules including growth factors, adhesion molecules, proteases and receptors and can support the functions of HS-binding molecules (Lindahl et al., 1998). HS chains are initially synthesised in the Golgi apparatus as polysaccharides consisting of tandem repeats of D-glucuronic acid (GlcA) and *N*-acetyl-D-glucosamine (GlcNAc). The nascent polysaccharides are subsequently modified in a series of steps: *N*-deacetylation/*N*-sulfation of GlcNAc, C5 epimerisation of GlcA to iduronic acid (IdoA), *O*-sulfation at C2 of IdoA and GlcA, *O*-sulfation at C6 of *N*-sulphoglucosamine (GlcNS) and occasional *O*-sulfation at C3 of GlcNS (Gallagher et al., 1992; Prydz and Dalen, 2000). *N*-deacetylation/*N*-sulfation, 2-*O*-, 6-*O*- and 3-*O*-sulfation of HS are mediated by the specific action of HS *N*-deacetylase/*N*-sulfotransferase (HSNDST), HS 2-*O*-sulfotransferase (HS2ST), HS 6-*O*-sulfotransferase (HS6ST) and HS 3-*O*-sulfotransferase, respectively (Lindahl et al., 1998; Prydz and Dalen, 2000). At each of the modification steps, only a fraction of the potential substrates are modified, resulting in considerable sequence diversity. This structural complexity of HS has made it difficult to determine its sequence and to understand the relationship between HS structure and function.

Recent evidence has indicated that HS is involved in various developmental processes interacting with important signalling molecules. Several biochemical studies have shown that fibroblast growth factors (FGFs) form a complex with GAG chains and that complex formation is essential for FGF-FGF receptor mediated mitogenesis (Rapraeger et al., 1991; Yayon et al., 1991; Turnbull et al., 1992; Ishihara, 1994; Pellegrini et al., 2000). Moreover, recent studies indicate important roles for sulfation of HS in developmental processes. *Drosophila* mutants in the gene *sulfateless*, encoding a homologue of vertebrate HSNDST, show abnormalities in Wingless-mediated dorsal/ventral patterning and FGF-dependent MAP kinase activation (Lin et al., 1999; Lin and Perrimon, 1999). Another *Drosophila* mutant in the homologue of HS2ST (*pipe*) shows abnormal dorsal/ventral polarity in the embryo (Sen et al., 1998). In vertebrates, transgenic mice that lack HS2ST die in the neonatal period showing abnormalities in the kidney, skeleton and eye development (Bullock et al., 1998).

Developing axons are guided to their appropriate targets by a succession of guidance molecules variously distributed along the pathway, which act as local cues to attract or repel the

growth cones of elongating axons (Tessier-Lavigne and Goodman, 1996). Some axon guidance molecules can bind to GAG chains in vitro. For instance, netrin-1 and netrin-2 were originally purified using heparin affinity columns (Serafini et al., 1994), suggesting that these guidance molecules might bind to HS in vivo. A netrin receptor, deleted in colorectal carcinoma (DCC), also binds to GAG chains in vitro (Bennett et al., 1997). Moreover, HS alters the characteristics of neurite outgrowth from neurons in vitro (Verna et al., 1989; Dow et al., 1991; Giuseppetti et al., 1994; Bandtlow and Zimmermann, 2000) and enhances slit2-mediated signalling in vitro (Hu, 2001).

Despite these studies, the GAGs involved in the axon guidance in vivo have not been characterised and little is known about the function of HS in axon guidance in vivo. In the developing *Xenopus* brain, retinal ganglion cell (RGC) axons extend through the diencephalon and cross the diencephalic/midbrain border to reach their primary target, the optic tectum (Chien et al., 1993). Using a live brain assay, we have previously shown that addition of HS exogenously causes striking misrouting of retinal axons at the tectal border (Walz et al., 1997) indicating that HS is involved in the axon targeting of the *Xenopus* optic pathway. Here we investigate the structural requirements of GAG chains that affect RGC axon targeting in vivo. We show that the axon targeting is disrupted by inhibition of HS sulfation. Using chemically modified heparins we also show that this disruption is related to the presence of specific sulfate groups, especially *O*-sulfates. Furthermore, experiments with purified heparin saccharides show that the disruption of axon targeting correlates with distinct saccharide structures. In addition, in situ hybridisation experiments for HS2ST and HS6ST suggest that expression patterns of these enzymes could be important for generating distinct HS structures in the dorsal diencephalon, which may be critical for repulsively steering axon growth into the tectum. This is the first report to show that specific HS structures are capable of differential effects on axonal navigation and the observations support the view that specific endogenous HS sequences are essential for the regulation of axon guidance signalling in the developing central nervous system.

MATERIALS AND METHODS

Materials

Sodium chlorate was purchased from Sigma. Porcine mucosal HS was obtained from Celsus (Cincinnati, Ohio, USA). Completely desulfated, *N*-sulfated heparin was from Seikagaku Corp. (Tokyo). Size-fractionated heparins (dp2-dp20) were prepared as described previously (Turnbull et al., 1999). The sources of other materials are indicated in the text.

Embryos

Embryos were obtained from adult *Xenopus laevis* injected with human chorionic gonadotropin. Embryos were raised in 0.1× MBS (8.8 mM NaCl, 0.1 mM KCl, 0.24 mM $NaHCO_3$, 82 μM $MgSO_4$, 33 μM $Ca(NO_3)_2$, 41 μM $CaCl_2$ and 1 mM Hepes, pH 7.5) at temperatures between 14°C and 25°C. Staging was according to the Nieuwkoop and Faber staging tables (Nieuwkoop and Faber, 1967).

Exposed optic pathway preparation and bypass phenotype

Exposed brain preparation experiments were performed as described previously (Chien et al., 1993). Stage 35/36 embryos were transferred to a Sylgard Petri dish and anaesthetized with 0.4 g/l MS222 (3-aminobenzoic acid ethyl ester methanesulphonate salt; Sigma) in 1× MBS. The embryos were immobilized by pinning and the skin, dura and eye were removed from the left side of the head, exposing the intact optic tract and tectum. The embryos were transferred to 1.3× MBS containing 0.1 g/l MS222 with or without various experimental reagents, and kept at 21°C during development to stage 40. To visualize the optic projection, the axons from the remaining right eye were labelled anterogradely with horseradish peroxidase (HRP; type VI; Sigma) and stained with diaminobenzidine as described previously (Cornel and Holt, 1992; Walz et al., 1997). Control retinal projections typically exhibit a 45° caudal bend in the optic tract and cross the diencephalic/midbrain border to enter the tectum (e.g. Fig. 1A). The bypass phenotype was characterized by a failure of most axons in the projection to cross the diencephalic/midbrain border (e.g. Fig. 1B,C). Within each experiment, the number of brains showing a bypass phenotype was counted and expressed as a percentage of the total number of brains.

Preparation of selectively desulfated heparins

All chemically modified heparin samples were produced from bovine lung heparin (Sigma). De-6-*O*-sulfated heparin was prepared as described (Yates et al., 1996) with slight modifications. Briefly, heparin was converted to the pyridinium salt, and desulfated in dimethyl sulphoxide/methanol (9/1, v/v) by heating at 50°C for 11 days. The polysaccharide was subjected to re-*N*-sulfation (Lloyd et al., 1971), and purified. Nuclear magnetic resonance (NMR) spectroscopy analysis indicated that the sample was de-*O*-sulfated at position 6 of GlcN in approximately 90% of residues. Some additional loss of *O*-sulfates from IdoA residues (approx. 20%) was also found. De-2-*O*-sulfated heparin was prepared using an alkaline treatment as described (Jaseja et al., 1989). The polysaccharide was subjected to re-*N*-sulfation (Lloyd et al., 1971) and characterised by NMR spectroscopy. De-*N*-sulfated/re-*N*-acetylated heparin was prepared and characterised as described (Yates et al., 2000). Heparin in which all free-hydroxyl groups were substituted with *O*-sulfates was prepared and characterised as described (Yates et al., 1996).

Preparation of partially desulfated heparins

De-2-*O*-sulfation

Bovine lung heparin was partially desulfated on IdoA residues by a modification of the methods described (Jaseja et al., 1989; Piani et al., 1993), in which IdoA residues were transformed into epoxide containing groups, thereby removing the sulfate groups. Samples were removed (after 60, 105, 195 and 480 minutes) from the reaction vessel, and characterised. The levels of de-2-*O*-sulfation are shown in Fig. 4C.

De-6-*O*-sulfation

Bovine lung heparin was de-6-*O*-sulfated and characterised by a modification of the method described (Yates et al., 1996). The pyridinium salt of heparin was heated at 50°C for various times (1, 3, 7, 11 days) and re-*N*-sulfated as described (Lloyd et al., 1971). Levels of 6-de-*O*-sulfation are shown in Fig. 4C.

Purification of heparin oligosaccharides with SAX-HPLC

Porcine mucosal heparin (Sigma) was partially digested by a combination of heparitinase I, II and III (Seikagaku). The digested oligosaccharide materials were applied to a SAX-HPLC column (Propac PA-1, 4×250 mm) and eluted with a linear gradient of NaCl (pH 7.0, 0-2 M, over 2 hours). Fractions were collected between 60 and 90 minutes and further separated with SAX-HPLC, eluting with a shallower linear gradient (NaCl pH 7.0, 0.8-1.3 M, for 3 hours). Several peaks were chosen, corresponding to those shown in Fig. 6B. The concentrations of NaCl required for their elution were: 0.87, 0.94, 0.99, 1.07 and 1.10 M, respectively.

Disaccharide composition analysis of the purified oligosaccharides was performed by modifications of the method described previously (Turnbull et al., 1999). Briefly, the purified oligosaccharides were depolymerised by mixed heparitinases. The resultant saccharides were tagged with 7-amino-1, 3-napthalene disulfonic acid (ANDSA, Fluka) as described (Drummond et al., 2001) and analysed by SAX-HPLC with reference to authentic standards (Seikagaku) labelled with ANDSA.

Isolation of cDNA clones for *Xenopus* HS2ST and HS6ST

Partial cDNA fragments (506 bp) for *Xenopus* HS2ST (Bullock et al., 1998) were amplified by RT-PCR.

To obtain a partial cDNA for *Xenopus* HS6ST, two oligonucleotide primers were synthesized on the basis of the mouse and human HS6ST cDNA sequences (Habuchi et al., 1998; Habuchi et al., 2000). PCR amplification was performed with a reverse-transcribed cDNA prepared from total RNA of *Xenopus laevis* embryos (stage 39) as a template, and the amplified DNA (199 bp) was sequenced. To clone a longer cDNA fragment, primers (5′-TGCTACAGACCCAACCG-AAAGGAGAC-3′ and 5′-TCNGTNAGNCCRAARAANGCCAT-3′) were synthesised based on the sequences of the mouse and human HS6ST cDNAs (Habuchi et al., 1998; Habuchi et al., 2000) and the 199-bp *Xenopus* fragment. PCR amplification was performed using the reverse-transcribed *Xenopus* cDNA, and the amplified PCR fragments were sequenced. One amplified clone was 474-bp long and showed 75% homology to the human HS6ST. The sequence of the 474-bp cDNA has been submitted to the DDBJ/EMBL/GenBank databases under accession number AB054535.

In situ hybridisation

Whole-mount in situ hybridisation was performed as described (Shimamura et al., 1994) with slight modifications. Digoxigenin-labelled RNA probes of *Xenopus* HS2ST and HS6ST were generated by in vitro transcription of the *Xenopus* HS2ST and HS6ST cDNA with SP6 or T7 RNA polymerase. Embryos (stage 39) were fixed with 4% paraformaldehyde in phosphate-buffered saline. The brains were dissected out of the embryos and subjected to in situ hybridisation. The hybridised probes were detected with anti-digoxigenin antibodies (Roche) and BM purple AP substrate (Roche). The retinal axons of the embryos hybridised with antisense HS6ST RNA were visualized with HRP before the hybridisation reaction.

RESULTS

Exogenous GAGs disrupt axon targeting

RGCs begin to extend their axons at stage 28 in *Xenopus*. The first retinal axons reach the optic chiasm at stage 32 and cross to the contralateral side of the brain. These axons then grow dorsally through the diencephalon to form the optic tract. The first axons enter the tectum at stage 37/38, and most of the retinal axons innervate the tectum by stage 40 (Holt, 1984).

To identify molecules involved in the RGC axon extension and targeting, we developed an exposed brain preparation in which the embryonic epidermis is removed and the underlying optic pathway is exposed to bath-applied drugs during the period of the RGC axon extension (Chien et al., 1993). Fig. 1A shows a typical axonal projection from the brain bathed in the control medium from stage 35/36 to 40, a period of approximately 16 hours. The RGC axons show normal extension as they extend through the diencephalon and cross the diencephalic/midbrain border to enter the tectum. We previously reported that brains exposed to GAGs showed abnormal axonal trajectories (Walz et al., 1997). When brains were exposed to 100 μg/ml of HS or heparin, a specific subclass of the HS family produced in mast cells (Turnbull et al., 2001), most retinal axons failed to cross from the diencephalon into the tectum, producing the ‘bypass’ phenotype (Fig. 1B,C). Bypass projections typically lacked a caudal bend in the mid-optic tract and frequently crossed over the dorsal midline of the diencephalon to enter the other side of the brain. The bypass phenotype was never induced in embryos bathed in the control medium. Exogenously applied heparin and HS do not affect the gross organization of the neuroepithelium or the main axon tracts (Walz et al., 1997). Digestion of endogenous HS by heparitinase treatment also caused the RGC projections to bypass the tectum (Walz et al., 1997). This indicates that the endogenous HS in *Xenopus* brain is important for the RGC axon targeting and that exogenous GAGs probably competitively interfere with interactions between endogenous HS and HS-binding molecules that are necessary for correct axonal navigation.

Sulfation of HS is necessary for RGC axon targeting

In dose-response experiments with exogenous GAGs, bovine lung heparin at a concentration of 1 μg/ml caused 85% of the projections to bypass the tectum (Fig. 2). When embryos were exposed to lower concentrations of heparin/HS, some axons

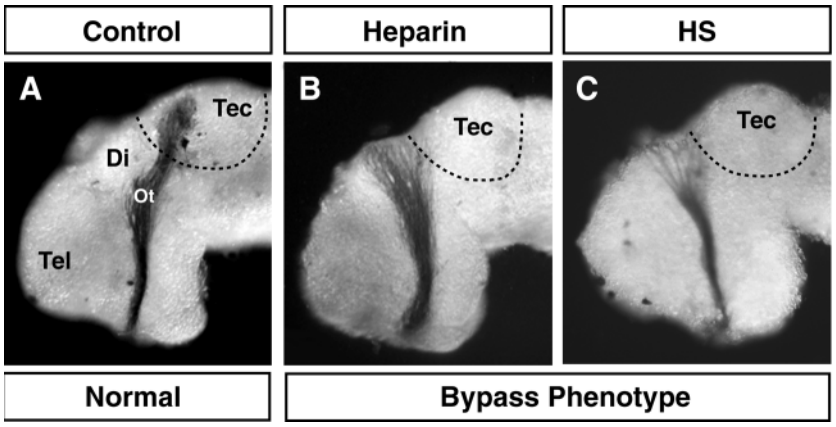

Fig. 1. Disruption of retinal axon targeting with exogenously applied GAGs. Lateral view of whole-mount brains at stage 40 showing the trajectories of HRP-filled optic projections. One side of the brain was exposed to GAGs from stage 35/36 to 40, the time when axons first grow from the mid-optic tract into the optic tectum (Tec). (A) Control projection showing HRP-filled axons coursing through the optic tract (Ot) in the diencephalon (Di) and crossing the diencephalon/midbrain boundary (dashed line anteriorly) into the tectum. Note the caudalward bend in the projection in the mid-optic tract. (B,C) Projections exposed to GAGs exhibiting the bypass phenotype. Brains were treated with 100 μg/ml of bovine lung heparin (B) and porcine mucosal HS (C), beginning when axons were in the mid-optic tract. The axons extend normally to the mid-optic tract, then take an aberrant route dorsally in the diencephalon, failing to cross the diencephalon/midbrain boundary, and bypass the tectum. Note the absence of a caudalward bend in the mid-optic tract. Tel, telencephalon; dorsal is up, anterior to the left.

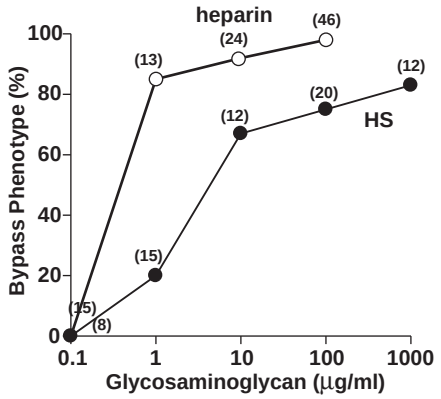

Fig. 2. Dose-response curves for the bypass phenotype induced by GAGs. Various concentrations of heparin (open circles) and HS (filled circles) were exogenously applied to exposed brains and plotted as a percentage of embryos showing the bypass phenotype. Numbers in parentheses indicate total number of embryos tested.

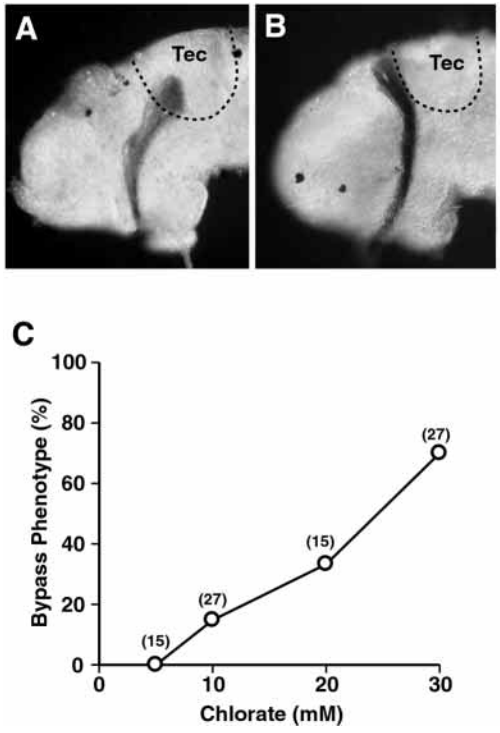

Fig. 3. Induction of the bypass phenotype by chlorate treatment. Chlorate was applied to exposed brains (stage 35/36 to 40) to inhibit the sulfation of endogenous HS. (A) Control projection crosses the diencephalon/midbrain boundary (dashed line anteriorly) to enter the anterior tectum (Tec). (B) Projection exposed to 30 mM of chlorate veers abnormally around the anterior border of the tectum and extends dorsally within the diencephalon. (C) Dose-response curve for the bypass phenotype induced with chlorate. The number of embryos exhibiting the phenotype is plotted as a percentage of the total number of embryos in each condition. Numbers in parentheses indicate total number of embryos per experimental condition.

bypassed the tectum and the others extended normally in a brain (data not shown). Porcine mucosal HS was less effective than heparin at inducing the bypass phenotype. Only 20% of embryos exposed to 1 μg/ml of HS showed the bypass phenotype; exposure to 10 μg/ml induced this phenotype in 67% of embryos but 1000 μg/ml of HS was needed to cause mistargeting in 83% of the brains (Fig. 2). While both heparin and HS consist of disaccharide repeats of alternating hexuronic acid (HexA, i.e. GlcA and IdoA) and glucosamine (GlcN) residues, heparin is more highly sulfated than HS (Lindahl et al., 1998). Bovine lung heparin is composed of approx. 90% of the repeating disaccharide IdoA(2S)-GlcNS(6S), with little GlcA and unsulfated IdoA (giving an average of almost 3 sulfates/disaccharide unit). In contrast, HS shows considerable structural heterogeneity, with much lower overall sulfation (approx. 1-2 sulfates/disaccharide unit) and distinct sulfated domains spaced apart by unsulfated regions (Turnbull et al., 2001). This raises the possibility that the different abilities of heparin and HS to induce the bypass phenotype (Fig. 2) depend on different levels of sulfation or, alternatively, the presence of different sulfated sequences in these GAGs.

To test the hypothesis that sulfation is essential for retinal axon guidance in *Xenopus*, exposed brains were treated with chlorate, an inhibitor of proteoglycan sulfation (Humphries and Silbert, 1988; Safaiyan et al., 1999). As shown in Fig. 3B, chlorate treatment induced the bypass phenotype in a dose-dependent way: 30 mM chlorate caused 70% mistargeting (Fig. 3C). Chlorate is also known to inhibit sulfation of chondroitin sulfate (CS) (Greve et al., 1988; Humphries and Silbert, 1988). However, when endogenous CS in the brain was digested by chondroitinase ABC treatment, RGC axons did not show a bypass phenotype (data not shown), suggesting that CS is not involved in *Xenopus* RGC targeting at the diencephalic/tectum border and that the chlorate-induced bypass phenotype is caused by the inhibition of HS sulfation. RGC axon crossing at the chiasm is disrupted by chondroitinase ABC treatment in mouse brain slices (Chung et al., 2000). The chiasm was not treated in our experiments, leaving open the possibility that CS is important at the chiasm in *Xenopus*. These results show that sulfate groups of HS are essential for its role in RGC navigation into the tectum.

Both 2-*O*- and 6-*O*-sulfate groups of HS are involved in axon pathfinding

Chlorate does not selectively reduce the formation of 2-*O*- and 6-*O*-sulfation on HS chains, and no selective inhibitor of 2-*O*- and 6-*O*-sulfation has been developed so far. To determine the requirement for specific sulfate groups of HS in axon targeting, we prepared selectively desulfated heparins and exogenously applied these modified heparins to exposed brains. We used heparin rather than HS as the source material for selective modifications, because heparin is more readily available than HS and is a potent bypass-inducer. Fig. 4B shows the dose-response curves for the chemically modified heparins at inducing the bypass phenotype. Intact heparin showed the highest level of the bypass phenotype induction, with an IC_{50} of 0.6 μg/ml. When *N*-sulfate groups were replaced by *N*-acetyl groups, the heparin derivative was only slightly less effective (IC_{50} of 1.5 μg/ml). In contrast, when 2-*O*- and 6-*O*-desulfated heparins were each assessed for their ability to induce the abnormal phenotype, these were much less effective. The IC_{50} values for the 2-*O*- and 6-*O*-desulfated heparins were 20 and

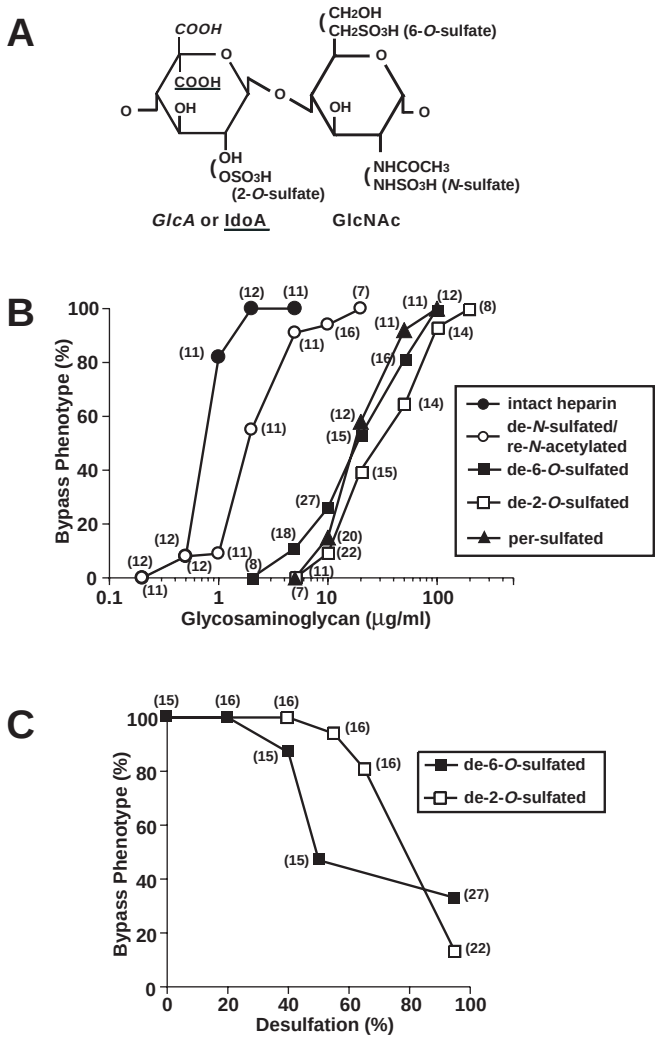

Fig. 4. Chemically modified heparin derivatives show differential bypass-inducing activities. (A) The structure of the disaccharide units in heparin and heparan sulfate. (B) Various concentrations of heparin derivatives were exogenously applied to exposed brains. Results are plotted as a percentage of embryos showing the bypass phenotype. The curves correspond to unmodified bovine lung heparin (filled circles), completely de-*N*-sulfated/re-*N*-acetylated heparin (open circles), completely de-6-*O*-sulfated heparin (filled squares), completely de-2-*O*-sulfated heparin (open squares), and per-sulfated heparin (filled triangles). (C) Partially de-2-*O*-sulfated heparin (open squares) and de-6-*O*-sulfated heparin (filled squares) were applied to exposed brains at 10 μg/ml. The percentage of the bypass phenotype induction is plotted against the degree of desulfation. Numbers in parentheses indicate total number of embryos.

30 μg/ml, respectively. Moreover, a heparin derivative that has *N*-sulfates but neither 2-*O*- nor 6-*O*-sulfates had little effect on axonal trajectories, even at higher concentration (14% bypass phenotype induction at 500 μg/ml; n=7). These results indicate that 2-*O*- and 6-*O*-sulfation are important for bypass phenotype induction, whereas *N*-sulfation probably plays only a minor role.

We also prepared various 2-*O*- and 6-*O*-desulfated heparins, which were partially desulfated to varying degrees, and tested them in the exposed brain assay. Progressive selective removal of 2-*O*- or 6-*O*-sulfate groups correlated with reduced potency to induce the bypass phenotype (Fig. 4C), although neither was absolutely required for activity (as seen in Fig. 4B). It is noteworthy, however, that the potency profiles for bypass-inducing activity for partially 2-*O*-desulfated and partially 6-*O*-desulfated heparins were not equivalent. We noted a sharp decrease in potency with removal of 40-50% of 6-*O*-sulfate groups (Fig. 4C). In contrast, approximately 70-80% of 2-*O*-sulfates needed to be removed before a significant loss of activity was observed (Fig. 4C). These results strongly indicate that the axon mistargeting is not a non-specific phenomenon caused by the net negative charges of the sulfate groups. In addition they suggest that there is a stringent requirement for particular sulfation patterns in heparin/HS in modulating axon navigation, with activity being particularly sensitive to the pattern of 6-*O*-sulfation.

When all free hydroxyl groups in the intact heparin were substituted with *O*-sulfates, this over-sulfated (‘per-sulfated’) heparin derivative showed a poor ability to induce the bypass phenotype, similar to that of the fully 6-*O*-desulfated and 2-*O*-desulfated heparin samples (Fig. 4B). Thus, higher sulfation density per se does not confer increased activity. This result probably reflects the involvement of other structural groups (such as hydroxyl groups) in molecular interactions with proteins that are involved in axon targeting; such groups would be blocked in per-sulfated heparin either directly by sulfate attachment or indirectly by the steric influence of additional sulfate groups.

Structural characteristics of oligosaccharides that disrupt RGC axon targeting

To determine in more detail the characteristics of GAG saccharides that are essential for inducing RGC axon mistargeting, we next ascertained the minimum size requirement of glycosaminoglycan chains. We prepared size-fractionated bovine lung heparin fragments, ranging from disaccharide (denoted dp2, where dp is degree of polymerisation, i.e. decasaccharide = dp10) to dp20. These were applied to exposed brains in vivo at 30 μM (approx. 100 μg/ml for dp10; Fig. 5A). Saccharides of dp6 or shorter showed only weak induction of the bypass phenotype, whereas the induction was moderately increased by treatment with dp8 to dp12 fragments. The strongest effects were observed with dp14 or longer fragments. Dose-response experiments for dp12 showed that 12.5 μM of dp12 caused 67% mistargeting (Fig. 5B). In contrast, dp6 showed only a weak effect even when used at a concentration of 50 μM, at which only 6% mistargeting was observed. These results show that a minimal size of approx. dp10 is required for efficient activity, though some activity persists even in smaller fragments.

We next purified some heparin oligosaccharides by strong-anion-exchange (SAX) HPLC to investigate the structural requirements for the bypass phenotype induction. Porcine mucosal heparin contains only approx. 60-70% of the trisulfated disaccharide (giving an overall average of approx. 2.5 sulfates/disaccharide unit) and displays much more sequence heterogeneity than bovine lung heparin. We therefore used porcine mucosal heparin as a source material to generate diverse saccharides by partial digestion employing a mixture of heparitinases, followed by SAX-HPLC purification (Fig. 6A,B). Five peaks from a small region of the separation profile

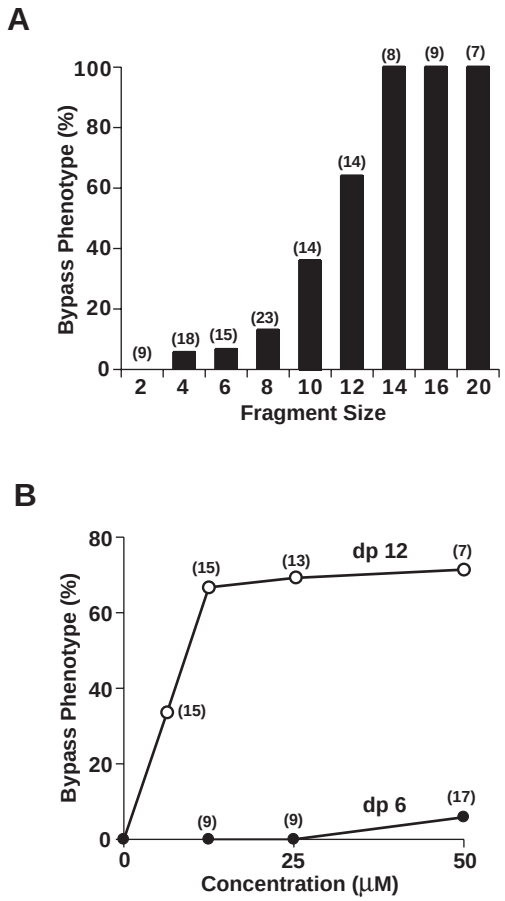

Fig. 5. Size-fractionated heparin oligosaccharides show different potencies for inducing the bypass phenotype. Exposed brains were treated with size-defined heparin oligosaccharides. (A) Size-dependency of heparin oligosaccharides to induce the bypass phenotype. Brains were exposed with 30 μM of size-fractionated bovine lung heparin fragments. (B) Dose-response curves for the bypass phenotype induction with dp6 (filled circles) and dp12 (open circles). Results are expressed as a percentage of total embryos showing the bypass phenotype. Numbers in parentheses indicate total number of embryos.

were selected according to elution position from the column (designated peaks 1-5). The sizes of the peaks determined by gel electrophoresis were similar to each other (dp8-10; data not shown). As shown in Fig. 6C, these peaks displayed differing abilities to induce the bypass phenotype, ranging from 10 to 100%. To assess the relationship between the mistargeting ability and the structures of these purified saccharides, we analysed their disaccharide compositions (Table 1). The stronger bypass-inducing activity in peaks 3-5 correlated with the proportions of HexA(2S)-GlcNS(6S) in these peaks, suggesting a strong association between mistargeting activity and the presence of both 2-*O*- and 6-*O*-sulfate groups. Peaks 1 and 2 showed weak mistargeting abilities and lacked 2-*O*-sulfates. These results suggest that the presence of 6-*O*-sulfates can confer higher bypass-inducing activity than 2-*O*-sulfates, although 2-*O*-sulfates clearly have a role in enhancing the activity. There was no correlation apparent between bypass-inducing activity and the level of *N*-sulfation. Furthermore, although peak 2 was less 6-*O*-sulfated than peak 1, peak 2 showed higher potency than peak 1. This suggests that non-*O*-sulfated disaccharides (HexA-GlcNAc and HexA-GlcNS) could contribute to bypass-inducing activity (perhaps by providing appropriate spacing between critical O-sulfate groups) and also that saccharide sequence is critically related to functional activity. This is consistent with the result of the exogenous application experiment with the per-sulfated heparin, which is less effective than the intact heparin for inducing the bypass phenotype (Fig. 4B). It is therefore clear that the mistargeting ability does not simply correlate with the level of sulfation, and that the differential abilities of the selected peaks are likely to be due to the different structural motifs they contain. Taken together, the exogenous application

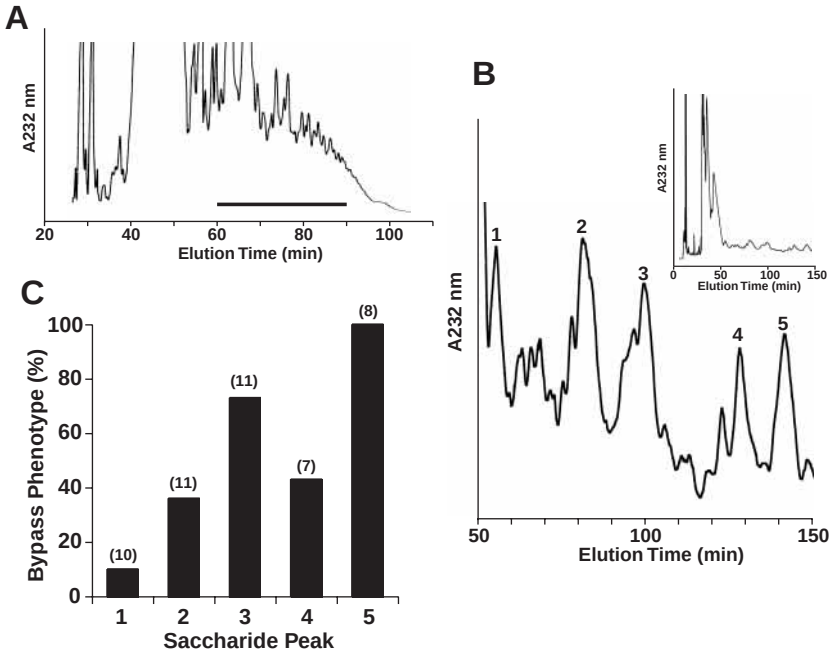

Fig. 6. Ability of purified heparin oligosaccharides to induce the bypass phenotype. (A,B) Purification of heparin oligosaccharides with SAX-HPLC. (A) Oligosaccharides derived by heparitinase treatment of porcine mucosal heparin were separated using SAX-HPLC with a linear NaCl gradient (0-2 M NaCl). Fractions collected between 60 and 90 minutes were combined. (B) The combined sample from A was further purified using SAX-HPLC with a shallower NaCl gradient (0.8-1.3 M NaCl), and peaks 1 to 5 were isolated. The inset shows the complete elution profile. (C) The ability of peaks 1 to 5 at a concentration of 10 μM to induce the bypass phenotype. Results are expressed as a percentage of total embryos showing the bypass phenotype. Numbers in parentheses indicate total number of embryos.

Table 1. Disaccharide composition of purified heparin oligosaccharides

	Peak				
Disaccharide structure	1	2	3	4	5
ΔHexA-GlcNAc	ND	10	8	12	16
ΔHexA-GlcNAc(6S)	18	26	20	5	6
ΔHexA-GlcNS	ND	10	ND	12	8
ΔHexA-GlcNS(6S)	82	54	24	33	15
ΔHexA(2S)-GlcNS	ND	ND	ND	8	ND
ΔHexA(2S)-GlcNS(6S)	ND	ND	48	30	55

Heparin oligosaccharides (peaks 1-5; Fig. 6B) were completely depolymerised using heparitinases, fluorescently labelled and resolved by SAX-HPLC. The compositions were expressed as a percentage of total disaccharides (ND, none detected). Heparitinase degradation results in modified disaccharides with Δ4, 5-unsaturated hexuronic acid residues (ΔHexA).

For abbreviations, see text.

experiments with the modified heparins and the purified heparin saccharides in vivo suggest that a combination of 2-*O*-sulfates, 6-*O*-sulfates and probably also non-sulfated groups of HS are intimately involved in *Xenopus* RGC axon pathfinding.

Expression pattern of HS2ST and HS6ST in embryonic brains

Since 2-*O*- and 6-*O*-sulfation are critical for the mistargeting activity of exogenous glycosaminoglycans, we next examined the expression patterns of HS2ST and HS6ST in the *Xenopus* embryonic brains by in situ hybridisation. *Xenopus* HS2ST cDNA was already cloned (Bullock et al., 1998). While human HS6ST and three mouse HS6ST isoforms, HS6ST1 (a homologue of the human clone), HS6ST2 and HS6ST3, have been cloned (Habuchi et al., 1998; Habuchi et al., 2000), *Xenopus* HS6ST has not been isolated yet. We hence isolated a partial cDNA clone for *Xenopus* HS6ST using RT-PCR with oligonucleotide primers based on the human and mouse HS6ST cDNA sequences. We obtained a *Xenopus* cDNA fragment of 474-bp, whose deduced amino acid sequence shows 86% homology to the human HS6ST protein (data not shown). A 47-amino-acid region (RKFYYITLLRDPVSRY-LSEWRHVQRGATWKTSLHMCDGRTPTPEELP) in the deduced *Xenopus* protein sequence is identical to the corresponding region of the human HS6ST (Habuchi et al., 1998), which contains the putative 3′-phosphoadenosine 5′-phosphosulfate binding site (RDPVSRYLS) for the donor substrate of HS6ST (Habuchi et al., 2000). This suggests the 474-bp cDNA is a partial fragment of *Xenopus* orthologue of HS6ST. The *Xenopus* cDNA fragment shows 75%, 54% and 72% homology to the mouse HS6ST1, HS6ST2 and HS6ST3 cDNA, respectively. Some regions of the *Xenopus* cDNA sequence are more homologous with the corresponding regions of the mouse HS6ST1 than HS6ST3, but the other regions of the *Xenopus* clone are more similar to the mouse HS6ST3 cDNA, suggesting that the *Xenopus* clone may be the counterpart of both HS6ST1 and HS6ST3. Moreover, we have isolated several clones from *Xenopus* and these clones encode the same protein. It is therefore possible that *Xenopus* does not have three HS6ST isoforms as mouse does.

We next conducted whole-mount in situ hybridisation with embryonic brains at stage 39, when the RGC axons begin to enter the tectum. HS2ST mRNA expression was detected widely in all regions of the brain, but stronger expression was observed in the posterior tectum, dorsal diencephalon and in the telencephalon (Fig. 7A). In marked contrast, the distribution of HS6ST mRNA was much more region-specific (Fig. 7B) with expression located exclusively in the telencephalon, dorsal diencephalon and in the posterior tectum. Significantly, the optic pathway occupies HS6ST-free territory and the dorsal border of the optic tract closely abuts the ventral border of HS6ST-expression in a manner that suggests exclusion of axon growth (Fig. 7B). By excluding growth into the dorsal diencephalon, 6-*O*-sulfated HS may play a repulsive role in steering axons across the diencephalic/midbrain border into the tectum. HS6ST is also absent in the anterior tectum where retinal axons terminate.

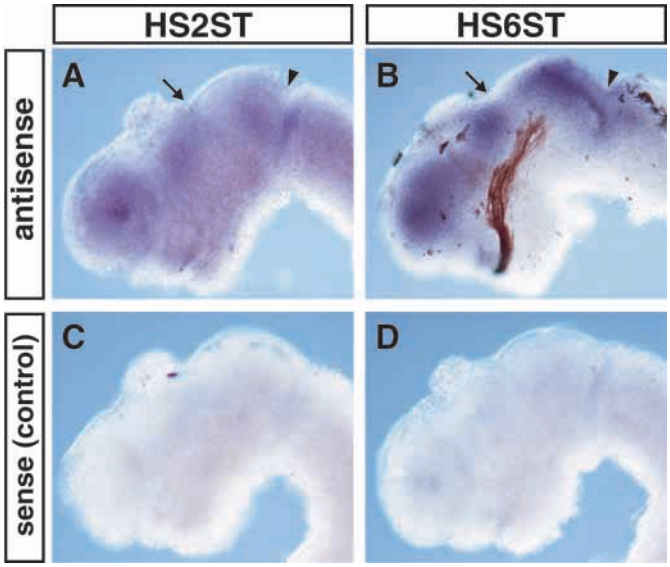

Fig. 7. Expression pattern of *Xenopus* HS2ST and HS6ST in the embryonic brain. (A,B) Lateral views of brains (stage 39) after whole-mount in situ hybridisation with antisense HS2ST (A) and HS6ST (B) RNA probes. Retinal axons are stained with HRP in (B). Arrows and arrowheads indicate the borders of the diencephalon/tectum and tectum/hindbrain, respectively. (C,D) Control embryos hybridised with sense probes.

DISCUSSION

The results presented here indicate that endogenous sulfated HS structures are essential for axon targeting at the diencephalic/tectum border in *Xenopus*. First, the embryos treated with chlorate, an inhibitor of HS sulfation, exhibit disrupted axon targeting. Second, exogenous application of selectively de-2-*O*- or de-6-*O*-sulfated heparin induces the bypass phenotype less effectively than intact heparin and correlations exist between sulfation and mistargeting activity, suggesting a requirement for sulfates at particular positions. However, the effect is not simply dependent on charge density; indeed, exogenous application of over-sulfated heparin shows a weaker ability to induce the bypass phenotype. Fourth, approx. dp8 to dp10 or longer saccharides are necessary for the activity. Fifth, it is clear that some oligosaccharides with different

structures are more potent inducers of the bypass phenotype than others. Finally, RGC axon extension in the dorsal optic tract closely follows along the border of the HS6ST-expressing area.

Recent studies using *Drosophila* mutants and transgenic mice indicate that sulfation of HS has important roles in developmental processes (Bullock et al., 1998; Sen et al., 1998; Lin et al., 1999; Lin and Perrimon, 1999). However, since HS interacts with various molecules that are essential for early morphogenesis, transgenic mice and *Drosophila* mutants that lack proper HS biosynthesis show multiple developmental defects. It has been difficult to study the role of HS in later developmental processes such as the formation of nerve connections, and the exposed brain assay used in this study has particular advantages for understanding the function of HS in RGC axon guidance in vivo. First, intact brains are exposed in a defined region and only for the short period of interest relevant for RGC axon pathfinding. Second, we can test various oligosaccharides in vivo, whereas previously they have been tested only in vitro. This system makes it possible to apply various oligosaccharides directly to the *Xenopus* brains in vivo. We have previously shown that the digestion of endogenous HS by heparitinase treatment in the *Xenopus* brain disrupts RGC axon targeting and causes the bypass phenotype (Walz et al., 1997). Inhibition of HS sulfation by chlorate treatment also induces the bypass phenotype. These results suggest that endogenous HS and sulfate groups of HS in the *Xenopus* brain are involved in axon guidance into the tectum. Exogenous application of GAGs and their derivatives induce the bypass phenotype, an effect which is presumably due to their ability to competitively inhibit the action of endogenous HS species (Walz et al., 1997). This idea is supported by a study on hepatocyte growth factor (HGF)-HS binding on rat hepatocytes (Naka et al., 1993). Exogenous heparin disrupts HGF-mediated signalling by competitively inhibiting the binding of HGF to endogenous HS rather than behaving as a cell-surface proteoglycan that activates HGF signalling. Unfortunately it is not yet feasible to purify the endogenous HS species from *Xenopus* embryonic brains and perform sequencing and functional analyses, owing to the small size of the brains. Nevertheless, the results of our in vivo experiments with exogenous GAGs are quantitatively reliable (e.g. Fig. 4), and allow assessment of the effects of specific exogenous structures on axon targeting. Our results demonstrate HS structural specificity in the induction of the bypass phenotype and represent the first step towards identifying the specific features of the endogenous HS species in *Xenopus* embryonic brain that influence axon targeting. Future developments in the field of HS structure-function analysis will make investigation of these molecules more tractable.

HS is known to interact with various proteins and it is plausible that HS-protein interactions are central to the role of HS as a regulator of RGC axon targeting. In this regard, the sulfate groups of HS are known to have a pivotal role in the molecular interactions with proteins. Ionic bonds between negatively charged groups (sulfates and carboxylic acids) and positively charged amino acid residues are the principal binding forces holding HS and proteins in a tight complex. This has been shown by X-ray crystallography studies on heparin-FGF and FGF-heparin-FGF receptor complexes (Faham et al., 1996; DiGabriele et al., 1998; Plotnikov et al., 1999; Pellegrini et al., 2000). Exogenous de-2-*O*- and de-6-*O*-sulfated heparin are dramatically less effective at inducing the bypass phenotype than intact heparin, and mistargeting activity correlates strongly with disaccharides containing both 2-*O*- and 6-*O*-sulfate groups. These results indicate that *O*-sulfate groups are important for the pathfinding. The experiments with the partially selectively desulfated heparins suggest a particularly strong dependence on the presence, and probably distribution pattern, of 6-*O*-sulfate groups, and the purified oligosaccharides that lack 2-*O*-sulfates show weak but significant bypass-inducing activity. Therefore, 2-*O*- and 6-*O*-sulfate groups may not contribute equally to pathfinding and the bypass phenotype is induced by oligosaccharides in a manner that depends on the presence and location of particular sulfate groups rather than just net negative charge. Furthermore, it is noteworthy that additional interactions with carboxyl and hydroxyl side groups on the sugar chains are also involved in HS-protein interactions (Faham et al., 1996; DiGabriele et al., 1998; Plotnikov et al., 1999; Pellegrini et al., 2000). The per-sulfated heparin shows weak mistargeting activity and non-*O*-sulfated disaccharides may contribute to mistargeting, suggesting that free hydroxyl groups of HS are also needed for the bypass induction, or that the additional sulfate groups act to sterically hinder its interactions with proteins. It is also possible that additional sulfation alters the conformational characteristics of the molecule (Yates et al., 2000). Furthermore, dp8 to dp10 or longer oligosaccharides induce the bypass phenotype, whereas saccharides dp6 or smaller had little effect, suggesting that the size of oligosaccharides is also important for the activity. Taken together, our results suggest that there is a stringent requirement for specific saccharide sulfation motifs in endogenous HS in the *Xenopus* brain, which confers the ability to modulate axon guidance. We further suggest that these specific forms may regulate the activity of specific axon guidance proteins.

An important goal of future studies will be the identification of the HS-binding molecules involved in these interactions. FGF-2 is one of the best-documented HS-binding molecules and we previously showed that exogenous application of FGF-2 to the *Xenopus* brain induced abnormal RGC axon trajectories around the diencephalic/tectum border (McFarlane et al., 1995). However, the FGF-treated axons can cross the border, and grow slightly in dorsal or ventral directions, showing that the abnormal phenotypes caused by exogenous heparin/HS and FGF-2 are not identical. Moreover, de-*N*-sulfated/re-*N*-acetylated heparin fails to bind to FGF-2 in vitro (Rusnati et al., 1994; Yamane et al., 1998), suggesting that the *N*-sulfate group of GAGs is essential for FGF-2-mediated signalling. In contrast, the *N*-sulfation is not crucial for induction of the bypass phenotype. Therefore it seems less likely that FGF-2 is involved in HS-mediated axonal crossing at the diencephalic/tectum border. Another class of candidate molecules is the netrins. These are secreted chemotropic axon guidance molecules (Tessier-Lavigne and Goodman, 1996; Culotti and Merz, 1998) and netrin-1 and netrin-2 were originally isolated with heparin affinity columns (Serafini et al., 1994). In addition, DCC, a netrin receptor, binds to heparin via its fibronectin type III domain in vitro (Bennett et al., 1997). These binding results indicate that HS may modulate netrin-DCC mediated axon guidance in vivo. *Xenopus* RGC growth cones respond to netrin-1 and

the response is mediated by DCC in vitro (de la Torre et al., 1997). *Xenopus* netrin-1 localises to the optic nerve head and attractively guides axons out of the eye (Höpker et al., 1999). However, application of function-blocking anti-DCC antibodies to exposed brains did not disrupt axon targeting (data not shown). Furthermore, *Xenopus* netrin-1 is expressed in the mid-diencephalon and posterior tectum, but not around the diencephalic/tectum border (de la Torre et al., 1997). These results suggest that the netrin-1-DCC interaction is not involved at the choice point for axon navigation at the diencephalic/tectum border. An additional candidate is slit-2, whose binding to its receptor is enhanced by HS in vitro (Hu, 2001), and acts as the guidance cue in the midline (Brose et al., 1999), though the function of slit-2 in *Xenopus* RGC targeting is not yet known. Future biochemical and expression cloning approaches using the information from the GAG structures identified here should help in the identification of the HS-binding protein(s) involved in RGC axon guidance at the diencephalic/tectum border. For example, the purified heparin saccharides with lower sulfation but high potency could be used to affinity-purify candidate molecules from brain extracts.

The molecular mechanisms that govern target entry are still poorly understood. The differential expression patterns of HS2ST and HS6ST suggest that HS biosynthesis in different brain regions may produce spatially specific HS structures with different sulfation patterns. Of particular interest is the observation that retinal axons normally extend in HS6ST-free/HS2ST-rich territory. Axons in the dorsal optic tract closely follow along the ventral border of the HS6ST-expressing region, giving the impression that the HS6ST-expressing dorsal diencephalon actively excludes axon growth. Indeed, it is in this region, the dorsal diencephalon, where retinal axons grow aberrantly in the presence of exogenous HS, indicative of the removal of an inhibitory signal. Thus, we suggest that a specific 6-*O*-sulfated HS expressed in the dorsal diencephalon provides a crucial component of a repulsive signal that prevents axons from growing dorsally in the diencephalon and helps to direct them to the diencephalic/midbrain border. Repulsive signalling is known to be a common mechanism in axon guidance (Tessier-Lavigne and Goodman, 1996; Keynes et al., 1997) and HS has been identified as a critical component of the repulsive barrier to axon extension that exists in the dorsal midline of the embryonic mouse midbrain (Garcia-Abreu et al., 2000). While the removal of a repulsive barrier along the dorsal edge of the optic tract may account for the abnormal dorsalward direction of growth of axons in the diencephalon, it does not explain why axons do not cross the border into the tectum in treated brains. This aspect of the phenotype is more consistent with the replacement of an attractive signal in the tectum with a repulsive one. Attractive guidance cues can be converted to repulsive ones by components of the extra cellular matrix, for example, laminin converts netrin-1 from an attractive to a repulsive signal for retinal axons (Höpker et al., 1999). One possibility, then, is that HS maintains an attractive signal in the tectum, but when it is removed or competitively inhibited, the signal becomes repulsive. Thus, endogenous HS may play two roles: (1) repel axon growth along the dorsal border of the optic tract and (2) maintain an attractive signal in the tectum.

It is not known whether HS modulates axon extension by binding directly to RGC axons, or indirectly by binding to axon guidance molecules, but knowledge of the HS structural specificity involved in axon guidance might allow screening and identification of candidate binding molecules through the use of affinity techniques.

Finding the core protein of HS involved in axon guidance might facilitate understanding of the role of HS in axon navigation. Interestingly, syndecan-2 and -3, transmembrane HS core proteins, are expressed in non-overlapping patterns in the *Xenopus* brain; syndecan-2 is exclusively expressed at the diencephalic/tectal boundary, whereas syndecan-3 is expressed in the diencephalon and tectum but not at the diencephalic/tectal boundary (Teel and Yost, 1996). These results suggest that these syndecans could be candidates of HS proteoglycan core protein glycanated with the HS chains involved in axon targeting.

In conclusion, we show that specific HS structures are capable of blocking axon targeting, suggesting that particular endogenous HS sequences are essential for the regulation of guidance cues in the developing central nervous system. These studies lay the foundation for future work on the precise molecular mechanisms by which HS regulates RGC axon guidance.

We would like to thank Prof. John T. Gallagher for advice and providing oligosaccharides for preliminary experiments. We very much appreciate Prof. William Harris's comments on the manuscript. We also thank Scott Guimond and Shin-ichi Ohnuma for helpful discussions, and Asha Dwivedy, Fanny Mann, Andrea Viczian, Zoe Scholefield and Kathy Drummond for technical advice and assistance. This work was supported by grants from the Medical Research Council (C.E.H. and J.E.T.), the Biotechnology and Biological Sciences Research Council (E.A.Y. and J.E.T.) and the Tokyo Metropolitan Institute of Medical Science (A.I.).

REFERENCES

Bandtlow, C. E. and Zimmermann, D. R. (2000). Proteoglycans in the developing brain: new conceptual insights for old proteins. *Physiol. Rev.* **80**, 1267-1290.

Bennett, K. L., Bradshaw, J., Youngman, T., Rodgers, J., Greenfield, B., Aruffo, A. and Linsley, P. S. (1997). Deleted in colorectal carcinoma (DCC) binds heparin via its fifth fibronectin type III domain. *J. Biol. Chem.* **272**, 26940-26946.

Brose, K., Bland, K. S., Wang, K. H., Arnott, D., Henzel, W., Goodman, C. S., Tessier-Lavigne, M. and Kidd, T. (1999). Slit proteins bind Robo receptors and have an evolutionarily conserved role in repulsive axon guidance. *Cell* **96**, 795-806.

Bullock, S. L., Fletcher, J. M., Beddington, R. S. and Wilson, V. A. (1998). Renal agenesis in mice homozygous for a gene trap mutation in the gene encoding heparan sulfate 2-sulfotransferase. *Genes Dev.* **12**, 1894-1906.

Chien, C. B., Rosenthal, D. E., Harris, W. A. and Holt, C. E. (1993). Navigational errors made by growth cones without filopodia in the embryonic Xenopus brain. *Neuron* **11**, 237-251.

Chung, K. Y., Taylor, J. S., Shum, D. K. and Chan, S. O. (2000). Axon routing at the optic chiasm after enzymatic removal of chondroitin sulfate in mouse embryos. *Development* **127**, 2673-2683.

Cornel, E. and Holt, C. (1992). Precocious pathfinding: retinal axons can navigate in an axonless brain. *Neuron* **9**, 1001-1011.

Culotti, J. G. and Merz, D. C. (1998). DCC and netrins. *Curr. Opin. Cell Biol.* **10**, 609-613.

David, G. (1993). Integral membrane heparan sulfate proteoglycans. *FASEB J.* **7**, 1023-1030.

de la Torre, J. R., Hopker, V. H., Ming, G. L., Poo, M. M., Tessier-Lavigne,

M., Hemmati-Brivanlou, A. and Holt, C. E. (1997). Turning of retinal growth cones in a netrin-1 gradient mediated by the netrin receptor DCC. *Neuron* **19**, 1211-1224.

DiGabriele, A. D., Lax, I., Chen, D. I., Svahn, C. M., Jaye, M., Schlessinger, J. and Hendrickson, W. A. (1998). Structure of a heparin-linked biologically active dimer of fibroblast growth factor. *Nature* **393**, 812-817.

Dow, K. E., Riopelle, R. J. and Kisilevsky, R. (1991). Domains of neuronal heparan sulfate proteoglycans involved in neurite growth on laminin. *Cell Tissue Res.* **265**, 345-351.

Drummond, K. J., Yates, E. A. and Turnbull, J. E. (2001). Electrophoretic sequencing of heparin/heparan sulfate oligosaccharides using a highly sensitive fluorescent end label. *Proteomics* **1**, 304-310.

Faham, S., Hileman, R. E., Fromm, J. R., Linhardt, R. J. and Rees, D. C. (1996). Heparin structure and interactions with basic fibroblast growth factor. *Science* **271**, 1116-1120.

Gallagher, J. T., Turnbull, J. E. and Lyon, M. (1992). Patterns of sulfation in heparan sulfate: polymorphism based on a common structural theme. *Int. J. Biochem.* **24**, 553-560.

Garcia-Abreu, J., Mendes, F. A., Onofre, G. R., De Freitas, M. S., Silva, L. C., Moura Neto, V. and Cavalcante, L. A. (2000). Contribution of heparan sulfate to the non-permissive role of the midline glia to the growth of midbrain neurites. *Glia* **29,** 260-272.

Giuseppetti, J. M., McCarthy, J. B. and Letourneau, P. C. (1994). Isolation and partial characterization of a cell-surface heparan sulfate proteoglycan from embryonic rat spinal cord. *J. Neurosci. Res.* **37**, 584-595.

Greve, H., Cully, Z., Blumberg, P. and Kresse, H. (1988). Influence of chlorate on proteoglycan biosynthesis by cultured human fibroblasts. *J. Biol. Chem.* **263**, 12886-12892.

Habuchi, H., Kobayashi, M. and Kimata, K. (1998). Molecular characterization and expression of heparan-sulfate 6-sulfotransferase. Complete cDNA cloning in human and partial cloning in Chinese hamster ovary cells. *J. Biol. Chem.* **273**, 9208-9213.

Habuchi, H., Tanaka, M., Habuchi, O., Yoshida, K., Suzuki, H., Ban, K. and Kimata, K. (2000). The occurrence of three isoforms of heparan sulfate 6-*O*-sulfotransferase having different specificities for hexuronic acid adjacent to the targeted *N*-sulfoglucosamine. *J. Biol. Chem.* **275**, 2859-2868.

Holt, C. E. (1984). Does timing of axon outgrowth influence initial retinotectal topography in Xenopus? *J. Neurosci.* **4**, 1130-1152.

Höpker, V. H., Shewan, D., Tessier-Lavigne, M., Poo, M. and Holt, C. (1999). Growth-cone attraction to netrin-1 is converted to repulsion by laminin-1. *Nature* **401**, 69-73.

Hu, H. (2001). Cell-surface heparan sulfate is involved in the repulsive guidance activities of Slit2 protein. *Nature Neurosci.* **4**, 695-701.

Humphries, D. E. and Silbert, J. E. (1988). Chlorate: a reversible inhibitor of proteoglycan sulfation. *Biochem. Biophys. Res. Commun.* **154**, 365-371.

Ishihara, M. (1994). Structural requirements in heparin for binding and activation of FGF-1 and FGF-4 are different from that for FGF-2. *Glycobiol.* **4**, 817-824.

Jaseja, M., Rej, R. N., Sauriol, F. and Perlin, A. S. (1989). Novel regio- and stereoselective modifications of heparin in alkaline solution. Nuclear magnetic resonance spectroscopic evidence. *Can. J. Chem.* **67**, 1449-1456.

Keynes, R., Tannahill, D., Morgenstern, D. A., Johnson, A. R., Cook, G. M., Pini, A. (1997). Surround repulsion of spinal sensory axons in higher vertebrate embryos. *Neuron* **18**, 889-897.

Kjellen, L. and Lindahl, U. (1991). Proteoglycans: structures and interactions. *Annu. Rev. Biochem.* **60**, 443-475.

Lin, X., Buff, E. M., Perrimon, N. and Michelson, A. M. (1999). Heparan sulfate proteoglycans are essential for FGF receptor signaling during *Drosophila* embryonic development. *Development* **126**, 3715-3723.

Lin, X. and Perrimon, N. (1999). Dally cooperates with *Drosophila* Frizzled 2 to transduce Wingless signalling. *Nature* **400**, 281-284.

Lindahl, U., Kusche-Gullberg, M. and Kjellen, L. (1998). Regulated diversity of heparan sulfate. *J. Biol. Chem.* **273**, 24979-24982.

Lloyd, A. G., Embery, G. and Fowler, L. J. (1971). Studies on heparin degradation. I. Preparation of (35 S) sulphamate derivatives for studies on heparin degrading enzymes of mammalian origin. *Biochem. Pharmacol.* **20**, 637-648.

McFarlane, S., McNeill, L. and Holt, C. E. (1995). FGF signaling and target recognition in the developing Xenopus visual system. *Neuron* **15**, 1017-1028.

Naka, D., Ishii, T., Shimomura, T., Hishida, T. and Hara, H. (1993). Heparin modulates the receptor-binding and mitogenic activity of hepatocyte growth factor on hepatocytes. *Exp. Cell Res.* **209**, 317-324.

Nieuwkoop, P. D. and Faber, J. (1967). *Normal Table of* Xenopus laevis *(Daudin)*. North-Holland, Amsterdam.

Pellegrini, L., Burke, D. F., von Delft, F., Mulloy, B. and Blundell, T. L. (2000). Crystal structure of fibroblast growth factor receptor ectodomain bound to ligand and heparin. *Nature* **407**, 1029-1034.

Piani, J., Casu, B., Marchi, E. G., Torri, G. and Ungarelli, F. (1993). Alkali induced optical rotation changes in heparin and heparan sulfates and their relation to iduronic acid containing sequences. *J. Carbohydr. Chem.* **12**, 507-521.

Plotnikov, A. N., Schlessinger, J., Hubbard, S. R. and Mohammadi, M. (1999). Structural basis for FGF receptor dimerization and activation. *Cell* **98**, 641-650.

Prydz, K. and Dalen, K. T. (2000). Synthesis and sorting of proteoglycans. *J. Cell Sci.* **113**, 193-205.

Rapraeger, A. C., Krufka, A. and Olwin, B. B. (1991). Requirement of heparan sulfate for bFGF-mediated fibroblast growth and myoblast differentiation. *Science* **252**, 1705-1708.

Rusnati, M., Coltrini, D., Caccia, P., Dell'Era, P., Zoppetti, G., Oreste, P., Valsasina, B. and Presta, M. (1994). Distinct role of 2-*O*-, *N*-, and 6-*O*-sulfate groups of heparin in the formation of the ternary complex with basic fibroblast growth factor and soluble FGF receptor-1. *Biochem. Biophys. Res. Commun.* **203**, 450-458.

Safaiyan, F., Kolset, S. O., Prydz, K., Gottfridsson, E., Lindahl, U. and Salmivirta, M. (1999). Selective effects of sodium chlorate treatment on the sulfation of heparan sulfate. *J. Biol. Chem.* **274**, 36267-36273.

Sen, J., Goltz, J. S., Stevens, L. and Stein, D. (1998). Spatially restricted expression of pipe in the Drosophila egg chamber defines embryonic dorsal-ventral polarity. *Cell* **95**, 471-481.

Serafini, T., Kennedy, T. E., Galko, M. J., Mirzayan, C., Jessell, T. M. and Tessier-Lavigne, M. (1994). The netrins define a family of axon outgrowth-promoting proteins homologous to C. elegans UNC-6. *Cell* **78**, 409-424.

Shimamura, K., Hirano, S., McMahon, A. P. and Takeichi, M. (1994). Wnt-1-dependent regulation of local E-cadherin and alpha N-catenin expression in the embryonic mouse brain. *Development* **120**, 2225-2234.

Teel, A. L. and Yost, H. J. (1996). Embryonic expression patterns of *Xenopus* syndecans. *Mech. Dev.* **59**, 115-127.

Tessier-Lavigne, M. and Goodman, C. S. (1996). The molecular biology of axon guidance. *Science* **274**, 1123-1133.

Turnbull, J., Powell, A. and Guimond, S. (2001). Heparan sulfate: decoding a dynamic multifunctional cell regulator. *Trends Cell Biol.* **11**, 75-82.

Turnbull, J. E., Fernig, D. G., Ke, Y., Wilkinson, M. C. and Gallagher, J. T. (1992). Identification of the basic fibroblast growth factor binding sequence in fibroblast heparan sulfate. *J. Biol. Chem.* **267**, 10337-10341.

Turnbull, J. E., Hopwood, J. J. and Gallagher, J. T. (1999). A strategy for rapid sequencing of heparan sulfate and heparin saccharides. *Proc. Natl. Acad. Sci. USA* **96**, 2698-2703.

Verna, J. M., Fichard, A. and Saxod, R. (1989). Influence of glycosaminoglycans on neurite morphology and outgrowth patterns in vitro. *Int. J. Dev. Neurosci.* **7**, 389-399.

Walz, A., McFarlane, S., Brickman, Y. G., Nurcombe, V., Bartlett, P. F. and Holt, C. E. (1997). Essential role of heparan sulfates in axon navigation and targeting in the developing visual system. *Development* **124**, 2421-2430.

Yamane, Y., Tohno-oka, R., Yamada, S., Furuya, S., Shiokawa, K., Hirabayashi, Y., Sugino, H. and Sugahara, K. (1998). Molecular characterization of *Xenopus* embryo heparan sulfate. Differential structural requirements for the specific binding to basic fibroblast growth factor and follistatin. *J. Biol. Chem.* **273**, 7375-7381.

Yanagishita, M. and Hascall, V. C. (1992). Cell surface heparan sulfate proteoglycans. *J. Biol. Chem.* **267**, 9451-9454.

Yates, E. A., Santini, F., De Cristofano, B., Payre, N., Cosentino, C., Guerrini, M., Naggi, A., Torri, G. and Hricovini, M. (2000). Effect of substitution pattern on 1H, 13C NMR chemical shifts and 1J(CH) coupling constants in heparin derivatives. *Carbohydr. Res.* **329**, 239-247.

Yates, E. A., Santini, F., Guerrini, M., Naggi, A., Torri, G. and Casu, B. (1996). 1H and 13C NMR spectral assignments of the major sequences of twelve systematically modified heparin derivatives. *Carbohydr. Res.* **294**, 15-27.

Yayon, A., Klagsbrun, M., Esko, J. D., Leder, P. and Ornitz, D. M. (1991). Cell surface, heparin-like molecules are required for binding of basic fibroblast growth factor to its high affinity receptor. *Cell* **64**, 841-848.